1996

Dynamic Characterization of Noise and Vibration Transmission Paths in Linear Cyclic Systems: Part II Experimental Validation

H. J. Kim
United Technologies Carrier

Dynamic Characterization of Noise and Vibration Transmission Paths in Linear Cyclic Systems: Part II — Experimental Validation

Han Jun Kim[†] and Young Man Cho[‡]
[†] *United Technologies Carrier, P.O. Box 4808 Carrier Parkway, Syracuse, NY 13221*
[‡] *United Technologies Research Center, 411 Silver Lane, MS 129-55, East Hartford, CT 06108*

Abstract

Linear cyclic systems (LCS) are a class of systems whose dynamic behaviors change periodically. The first part of this two-part paper derives a generic expression that describes how the noise and/or vibration are transmitted between two (or multiple) points in LCS. In Part II, some experimental results validate the theoretical development in Part I. Noise and vibration transmission paths of scroll and rotary compressors (two typical LCS) are examined to show that LCS indeed generate a series of amplitude modulated input signals at the output, where the carrier frequencies are harmonic multiples of LCS' fundamental frequency. The criterion proposed in Part I to determine how well LCS can be approximated as linear time-invariant systems (LTIS) is applied to the noise and vibration transmission paths of the two compressors.

1 Introduction

It has become an overwhelming industry trend to eliminate or reduce the noise and vibration from dynamic systems via various routes such as product redesign, passive damping, active control of noise and vibration, etc. [1, 2, 3]. The first step toward noise/vibration reduction is to understand the mechanism(s) of noise/vibration generation and transmission and then to locate the noise/vibration sources and transmission paths. Numerous papers have dealt with these issues [4, 5, 6, 7, 8] and have been quite successful in identifying noise/vibration sources and transmission paths. For a subclass of general dynamics systems, linear cyclic systems (LCS), Part I of this two-part paper derives 1) a generic expression describing the interaction between the sources and transmission paths 2) a criterion used to classify LCS into genuine linear cyclic systems (GLCS) and pseudo linear cyclic systems (PLCS)/linear time-invariant systems (LTIS).

In Part II, the theoretical developments in Part I are validated with experimental results on a couple of cyclic systems, scroll and rotary compressors. In Part II, the noise/vibration sources and their interactions with the transmission paths in the two compressors are understood on the framework of the theoretical developments in Part I. Even though the fundamental mechanisms of generating noise/vibration are nonlinear, the transmission paths of the compressors can well be approximated as linear and cyclic in that 1) the noise/vibration sources are defined as nonlinear phenomena such as impact, gas discharge, etc. 2) the transmission paths themselves consist of rigid bodies 3) the compressor motions are approximately synchronized with the 60 Hz power line. Once the basic LCS assumption on the transmission paths is satisfied, the predictions made on LCS in Part I are verified with experimental data. The two compressors are shown to produce amplitude modulated input signals at the output along the reverse path that is used in the reciprocity experiment [8]. In addition, the experimental results support the claim in Part I that the phases of sideband signals are not synchronous with that of the output signal at the excitation frequency and are related to the angular position at the instant of excitation. The sideband criterion is applied in order to classify the two compressors. Both the compressors turn out to be PLCS. The implications of the classifications on signal processing techniques for noise/vibration sources and transmission paths are briefly discussed.

Section 2 presents experimental validation with a scroll compressor. Various theoretical developments in Part I are verified, and the scroll compressor is classified as a PLCS. Section 3 follows the outline of Section 2 but describes the experimental validation with a rotary compressor. The rotary compressor is also classified as a PLCS. The purpose of the experiments and analyses in Sections 2 and 3 are three-fold: 1) an LCS produce amplitude modulated input signals at the output 2) the phases of sideband signals are dependent upon the angular position of an LCS 3) the sideband criterion is applied to classify the two compressor into a PLCS or GLCS.

2 Experimental Validation with a Scroll Compressor

In this section, the analysis in Part I of this paper is validated with experimental data obtained from a scroll compressor. The tested scroll compressor is plugged into the 60 Hz power line and is driven by an AC motor which is

synchronized with the power line. As a result, the mechanical vibration and acoustic radiation from the compressor are synchronized with the motor speed and consist of the harmonics of the motor speed.

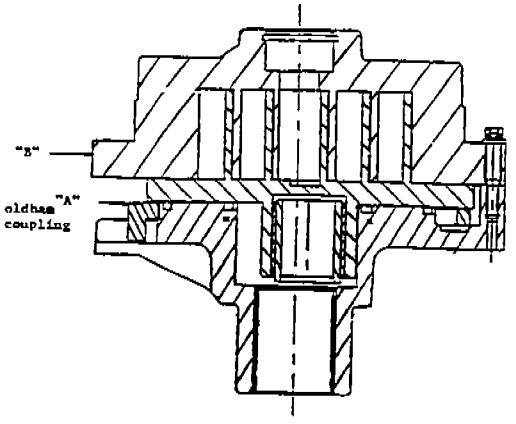

Figure 1: The scroll compressor instrumentation diagram.

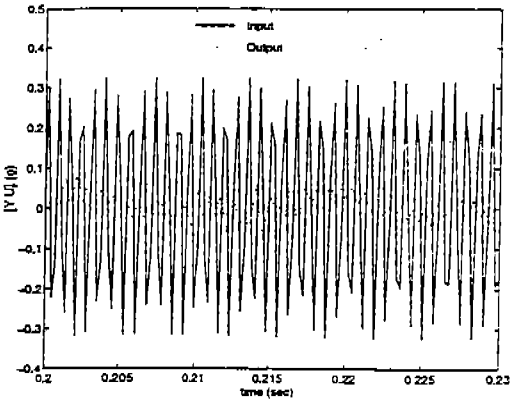

Figure 2: A snapshot of the input and output time series. The excitation frequency is 1262 Hz.

The scroll compressor is instrumented both internally and externally (overall two sensors) as shown in Figure 1. The internal one is located near the Oldham coupling and the external one is placed on the shell. The internal transducer 'A' measures both induced vibration (by the external force transducer) and intrinsic vibration (by the running compressor). The external transducer 'B' is a force transducer measuring the applied force. A sinusoid is chosen as the forcing function in order to take advantage of a frequency domain experiment as explained in Section 5. Part I of this two part paper. The HP spectrum analyzer is used throughout the experiment to 1) generate the forcing function 2) collect the sensor readings 3) record the measured data. In the following discussion, the external force transducer is assumed to be an input transducer and the internal accelerometer is assumed to be an output transducer since the vibration due to the force is transmitted from outside to inside through the running compressor, even if the compressor generated vibration is transmitted from inside to outside. Multiple sets of experiments are conducted with different excitation frequencies at the external force transducer. In this paper, only three representative sets are presented and discussed in detail. A time series of each transducer measurement is recorded at the sampling frequency 32.768 kHz. Each record is 40,960 samples long.

Figure 2 shows a snapshot of the input/output time series. The input signal is close to a pure sinusoid and the output signal contains various harmonics. This is manifested in Figure 3, where the input/output frequency spectra are shown. The input frequency spectrum contains only one sinusoid, while the output frequency spectrum shows the various harmonics of the compressor fundamental frequency and the harmonics of the input excitation that are marked with '*' in Figure 3.

The first experiment is conducted with the sinusoid forcing at 1262 Hz. The data are prefiltered and then subsampled at 4096 Hz. The subsampled waveform is subsequently truncated to give 2048 samples long snapshot, starting at those time instants when the input sinusoid crosses zero positively. The total of four snapshots are obtained from the subsampled waveform. Table 1 shows the magnitudes and phases of the input and output measurements at (the excitation frequency $\pm$ harmonic multiples of the compressor fundamental frequency), where only significant terms are shown. The magnitude and phase of the input signal do not change much as expected, since each snapshot is chosen to start at its positive zero-crossing instant. *The amplitude modulated input signals are clearly observed at the output (the accelerometer 'A'), which verifies the prediction in Part I. The carrier frequencies are harmonic multiples of the rotation speed of the compressor.* As also predicted by the theoretical discussion in Part I, neither do the magnitudes of the harmonics change much, nor do the phases at the excitation frequency $A_0(1262)$. On the other hand, the phases of A_k at $k \neq 0$ change significantly from snapshot to snapshot. *This is due to the different crankcase angles for different snapshots.*

To further validate the developed theory, the same experiments are conducted at two different frequencies: 2598 and 3773 Hz. Similar analyses are carried out for these two experiments. The results are shown in Tables 2 and 3. Similar conclusion can be drawn from these figures to those of the experiment at 1262 Hz.

Snapshot	1	2	3	4
Magnitude	322	322	322	322
Phase Angle	-64.3	-64.4	-64.5	-64.7

(a)

	1	2	3	4
1146	0.816	0.714	0.873	0.895
1204	0.780	1.00	0.659	0.945
1262	17.5	17.6	17.6	17.5
1322	0.841	0.518	0.331	0.597
1380	0.866	0.790	0.800	1.01

(b)

	1	2	3	4
1146	-42.9	117	98.8	77.2
1204	148	59.5	-140	30.9
1262	67.9	67.8	68.2	67.8
1322	-128	-38.7	140.3	-72.8
1380	129	-35.4	-18.5	17.7

(c)

Table 1: (a) The magnitudes and phase angles of four different input snapshots at 1262 Hz. Each contains 2048 samples at the sampling frequency 4096 Hz. (b) The magnitude responses of four corresponding outputs at five different harmonic frequencies. (c) The corresponding phase responses.

Snapshot	1	2	3	4
Magnitude	198	198	197	197
Phase Angle	145	145	145	145

(a)

	1	2	3	4
2483	6.28	6.53	7.39	7.79
2541	4.71	4.58	4.35	4.92
2598	31.9	31.9	31.3	31.6
2659	2.02	2.06	1.62	2.14
2717	0.951	0.387	0.228	0.677

(b)

	1	2	3	4
2483	-162	39.1	47.6	-99.6
2541	-74.1	24.2	-141	-40.2
2598	-42.2	-42.8	-41.7	-42.2
2659	-171	102	-102	167
2717	150	-72.3	-87.4	110

(c)

Table 2: (a) The magnitudes and phase angles of four different input snapshots at 2598 Hz. Each contains 2048 samples at the sampling frequency 6554 Hz. (b) The magnitude responses of four corresponding outputs at five different harmonic frequencies. (c) The corresponding phase responses.

Snapshot	1	2	3	4
Magnitude	1020	1020	1020	1020
Phase Angle	155	155	156	156

(a)

	1	2	3	4
3657	44.2	43.4	43.3	43.8
3716	6.01	5.26	4.23	4.41
3773	172	171	171	171
3832	7.93	8.74	9.74	8.70
3893	3.77	4.54	3.34	4.33

(b)

1	2	3	4	
3657	66.1	-10.5	-85.7	-23.2
3716	153	125	92.6	110
3773	165	166	166	166
3832	-153	-112	76.8	-104
3893	-116	21.7	-173	-75.5

(c)

Table 3: (a) The magnitudes and phase angles of four different input snapshots at 3773 Hz. Each contains 8192 samples at the sampling frequency 10,923 Hz. (b) The magnitude responses of four corresponding outputs at five different harmonic frequencies. (c) The corresponding phase responses.

Now the sideband criterion is applied to classify the scroll compressor. The sideband criterion states that the system under consideration is a PLCS if the following condition is satisfied: for the sideband amplitude response $A_k(f)$,

$$\int_{-\infty}^{\infty} [\sum_{k\neq 0} |A_k(f)|]^2 df < \rho\alpha \int_{-\infty}^{\infty} \sum_{k=-\infty}^{\infty} |A_k(f)|^2 df, \tag{1}$$

where the risk factor ρ is included. The sideband criterion can be evaluated only with several frequency points as far as they are representative of the whole frequency band of interest in terms of the relative sideband energy compared to the response signal energy at the excitation frequency. Now, we approximate (1) for the selected three frequency points $1262, 2598, 3773$ using $A_k(f)$ estimates in Table 1 (b), Table 2 (b) and Table 3 (b). The critical number α and the risk factor are chosen to be 0.2 (or 7 dB) and 1.5, respectively. The $A_k(f)$ estimates from the tables must be normalized with the corresponding input amplitudes in Table 1 (a), Table 2 (a) and Table 3 (a) before (1) is evaluated. Only $A_k(f)$ estimates of the first snapshot in each table are used.

$$\text{(LHS)} = \int_{-\infty}^{\infty} [\sum_{k\neq 0} |A_k(f)|]^2 df \approx 8.76 \cdot 10^{-3},$$

$$\text{(RHS)} = 1.5\,\alpha \int_{-\infty}^{\infty} \sum_{k=-\infty}^{\infty} |A_k(f)|^2 df, \approx 1.82 \cdot 10^{-2}.$$

$$\Longrightarrow \text{(LHS)} < \text{(RHS)}.$$

As a result, we can conclude that the scroll compressor is a PLCS/LTIS with the critical value 0.2. The variation energy of the impulse response is less than than 20 % of its average energy.

Now that the scroll compressor is classified as a PLCS/LTIS, the signal processing techniques for LTIS are viable tools for the compressor noise/vibration analysis. Two signal processing techniques have been considered for this purpose: reciprocity experiment and system identification. Both techniques were successful in identifying the noise/vibration sources and transmission paths.

3 Experimental Validation with a Rotary Compressor

This section validates the analysis in Part I with experimental data collected from a rotary compressor. The rotary compressor is plugged into 60 Hz power line and is driven by an AC motor synchronized with the power line. The experiments are conducted to verify the predictions based on the theoretical development in Part I and classify the rotary compressor (into a GLCS or a PLCS).

The rotary compressor is also instrumented both internally (one sensor) and externally (one sensor) as shown in Figure 4. The external transducer (a force transducer) is located vertically 1 cm up from the base of the compressor and horizontally 5 cm from the suction pipe. The internal transducer (an accelerometer) is at the opposite side of the compressor. The internal transducer measures vibration due to both the external force transducer and the running compressor. The experimental equipment and scheme in Section 2 are adopted here and, as a result, are not explained in detail for terseness except for the difference. The frequency range of interest in the rotary compressor experiment is 4500–6000 Hz, where the vibration of the rotary compressor are shown to be most active. Although multiple sets of experiments are conducted, only two of them are described here when the compressor is excited at 5060 Hz and 5460 Hz. A time series of each transducer is recorded at 16384 Hz to give a total of 60416 data points. The input/output snapshots are very similar to the one shown in Figures 2 and 3 and are not shown here.

The experimental data are truncated to give four 8192 samples long snapshots, starting at those time instants when the input sinusoid crosses zero positively. Tables 4 and 5 show the magnitudes and phases of only significant sideband signals at the output. It is clear that *the amplitude modulated input signals are observed at the output* (the accelerometer 'A'). The magnitudes of the harmonics $A_k(f)$ do not vary much from snapshot to snapshot, while *the phases do vary randomly except for the phases of the harmonic signals at the excitation frequency which is constant.*

Now the sideband criterion is applied to classify the rotary compressor. The frequency range of interest is 4.5–6 kHz, where most of the vibration energy is concentrated. As in the case of the scroll compressor in Section 2, the sideband criterion is evaluated with only a few frequency points, 5060 and 5460, to be precise. Now, we approximate (1) for the selected two frequency points using $A_k(f)$ estimates in Table 4 (a), and Table 5 (a). The critical number

	1	2	3	4
4994	40.8	33.2	35.9	46.6
5002	22.8	19.7	24.2	23.5
5060	510	513	498	501
5118	22.8	28.0	20.0	25.4
5176	18.6	22.6	22.9	15.7

(a)

	1	2	3	4
4994	109	128	-161	28.6
5002	-5.5	13.5	55.0	168
5060	170	172	170	172
5118	89.0	91.3	41.0	-99.5
5176	169	153	136	-32.4

(b)

Table 4: (a) The magnitude responses of four output snapshots at five different harmonic frequencies. (b) The corresponding phase responses.

	1	2	3	4
5344	19.2	18.8	17.3	18.7
5402	8.21	6.78	4.95	6.04
5460	435	434	431	433
5518	30.5	29.8	32.1	29.8
5576	13.5	16.2	15.6	17.7

(a)

	1	2	3	4
5344	-111	-170	176	140
5402	156	119	100	90.7
5460	111	110	110	110
5518	-124	-90.2	-76.8	-61.4
5576	-19.2	40.0	53.9	88.6

(b)

Table 5: (a) The magnitude responses of four output snapshots at five different harmonic frequencies. (b) The corresponding phase responses.

α and the risk factor are chosen to be 0.2 (or 7 dB) and 1.5, respectively. The $A_k(f)$ estimates from the tables are pre-normalized ones with the corresponding input amplitudes so that (1) can be directly evaluated without further normalization. Only $A_k(f)$ estimates of the first snapshot in each table are used.

$$(\text{LHS}) = \int_{-\infty}^{\infty} [\sum_{k \neq 0} |A_k(f)|]^2 df \approx 1.61 \cdot 10^4,$$

$$(\text{RHS}) = 1.5\,\alpha \int_{-\infty}^{\infty} \sum_{k=-\infty}^{\infty} |A_k(f)|^2 df, \approx 1.39 \cdot 10^5.$$

$$\Longrightarrow (\text{LHS}) < (\text{RHS}).$$

The comparison between the scroll compressor and the rotary compressor discloses interesting similarities and differences in their noise/vibration transmission path dynamics. They are similar in that 1) both of them exhibit the characteristics of LCS such as amplitude modulation effect, randomness of the sideband signal phases.etc. 2) both of them belong to PLCS, which is verified by the sideband criterion. Roughly speaking, these similarities in their responses can be traced to their structural similarity (rotating parts within a rigid body). The most conspicuous difference is the level of sideband signals, which also leads to the different ratios between the variation energy and the average energy. In Section 2, the application of the sideband criterion shows that the ratio between the variation energy and the average energy is $9.62 \cdot 10^{-2}$, where the risk factor is included. On the other hand, the corresponding ratio of the rotary compressor is $2.31 \cdot 10^{-2}$, where the risk factor is also included. Above analysis shows that the transmission path(s) of the scroll compressor varies more as a function of the crankcase angle θ than that of the rotary compressor. A careful comparison between the compressor structures unveils the following two causes that may contribute to such a significant discrepancy.

1. Figure 1 shows that the scroll compressor has a *direct* noise/vibration transmission path between the internal and external transducers since the fixed scroll and orbiting scroll are always in contact with each other in addition to the indirect path around the compressor shell. On the contrary, Figure 4 shows that there does not always exist a direct noise/vibration transmission path between (or across) the internal and external transducers

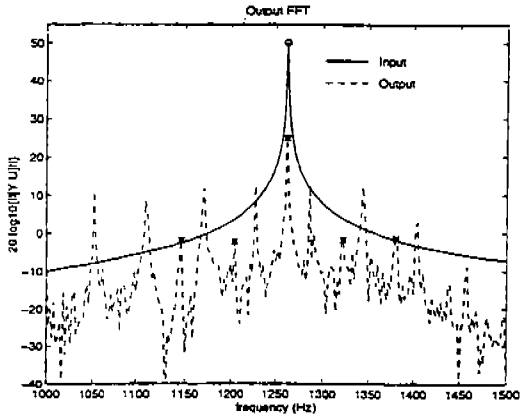

Figure 3: The magnitude response of the input and output time series. The excitation frequency is 1262 Hz.

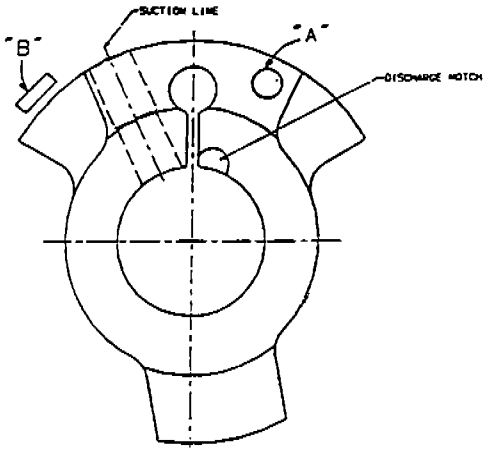

Figure 4: The rotary compressor instrumentation diagram.

in the rotary compressor. The noise/vibration is conjectured to be primarily transmitted around the compressor shell.

2. There exists a gap in the rotary compressor between the rotor and the shell which may play as a noise/vibration absorber.

4 Concluding Remarks

A linear cyclic system is shown 1) to produce amplitude modulated input signals whose carrier frequencies are harmonic multiples of the system's fundamental frequency 2) to generate sideband signals whose phases are dependent upon the crankcase angle of the system, via experimental validation on a scroll compressor and a rotary compressor. In addition, the sideband criterion proposed in Part I is applied to classify the scroll and rotary compressors as PLCS/LTIS, which makes signal processing techniques for LTIS viable tools for the noise/vibration source and transmission path identification in the scroll and rotary compressors. Although restricted to the two compressors. the approach and analysis in this paper may well be valid for other LCS, e.g. automobile engine.

References

[1] L. L. Faulkner, *Handbook of Industrial Noise Control*, Industrial Press Inc., New York, NY, USA, 1976.

[2] J. S. Bradley, "Disturbance caused by residential air conditioner noise", *J. Acoustic. Soc. Am.*, vol. 94, 1993.

[3] D. G. Smith, M. F. Arnold, Jr. E. W. Ziegler, and M. Brown, "A systems approach to appliance compressor quieting using active noise control techniques", in *In Proc. International Compressor Engineering Conference*, Purdue Univ., West Lafayette, IN, USA, 1992.

[4] R. W. Barker and M. J. Hinich, "Statistical monitoring of rotating machinery by cumulant spectral analysis", in *Proc. of the SPIE*, San Diego, CA, USA, July 1994, vol. 2296, pp. 43–51.

[5] Qingfeng Meng and Liangsheng Qu, "Rotating machinery fault diagnosis using wigner distribution", *Mechanical Systems and Signal Processing*, vol. 5, no. 3, pp. 155–166, May 1991.

[6] K. N. Lou, P. J. Sherman, and D. E. Lyon, "System identification and coherence analysis in the presense of a harmonic signal", *Mechanical Systems and Signal Processing*, vol. 7, no. 1, pp. 13–27, January 1993.

[7] S. Rantala and R. Suoranta, "Enhanced vibration monitoring using parametric modelling technique", in *In Proc. of IEEE Intrumentation and Measurement Technology Conference*, Atlanta, GA, USA, May 1991.

[8] T. ten Wolde, *Reciprocity Experiments on the Transmission of Sound in Ships*, PhD thesis, Delft University, 1973.